Toxicology Research

PAPER

Check for updates

Cite this: *Toxicol. Res.*, 2017, **6**, 342

Zinc oxide nanoparticle induced age dependent immunotoxicity in BALB/c mice

Violet Aileen Senapati,[a] Govind Sharan Gupta,[a] Alok Kumar Pandey,[b] Rishi Shanker,[a] Alok Dhawan *[b] and Ashutosh Kumar*[a]

Received 7th December 2016,
Accepted 13th March 2017

DOI: 10.1039/c6tx00439c

rsc.li/toxicology-research

Zinc oxide (ZnO) nanoparticles (NPs) have potential applications in cosmetics, food packaging and biomedicine but concerns regarding their safety need to be addressed. In the present study, the immunotoxic potential of ZnO NPs was evaluated in different ages of BALB/c mice after sub-acute exposure. The cytokine release, immunophenotyping, distribution of ZnO NPs and ultrastructural changes were assessed. A significant ($p < 0.05$) change in the CD4- and CD8-cells, levels of IL-6, IFN-γ and TNF-α and reactive oxygen species were observed in aged mice. In juvenile mice, increase in reactive oxygen species and IL-6 and TNF-α levels was observed with no significant changes in adult mice. A significant ($p < 0.05$) increase in the expression levels of mitogen activated protein kinase (MAPK) cascade proteins such as phospho-ERK1/2, phospho-JNK and phospho-p38 were also induced in aged mice. Collectively, our results indicate that the aged mice are more susceptible to ZnO NP induced immunotoxicity.

Introduction

The unique physicochemical properties of nanoparticles (NPs) accounts for their increased applications in drug delivery, imaging, cosmetics, paints, food industry, *etc.*[1] However when particles are reduced to the nano range, the reactivity increases due to increase in the surface area.[2] The increase in reactivity can lead to an increase in toxicity thereby raising concerns on the usage of NPs.[3]

Zinc oxide (ZnO) NPs are one of the most widely used NPs in consumer products including cosmetics, pharmaceutical and paint industries. ZnO NPs provide protection from ultraviolet A and B radiation due to their high absorption and reflective properties, hence they are used in sunscreens and paints.[4] ZnO NPs are also used as an anticancer therapeutic agent due to their photodynamic effect.[5]

Several studies of ZnO NPs *in vitro* have determined their cytotoxicity, cell membrane damage, increase in the levels of intracellular calcium, lipid peroxidation, oxidative DNA damage, expression of genes that are involved in apoptosis and oxidative stress responses.[6–8] However, *in vitro* models alone are insufficient to predict possible hazards to humans due to limited cell–cell communication and unavailability of the cell matrix which is otherwise possible in a co-culture experimental setup.[9–11] The *in vivo* evaluation of NP toxicity provides for a short-term or a long-term exposure with different routes of administration of NPs in organisms.[12] Hence, *in vivo* studies are necessary to elucidate the effect, mechanisms, pathways and entry routes of NPs in a complex multicellular organism. Previous *in vivo* studies in mice have shown that on exposure, NPs get deposited in organs of the immune system such as spleen and lymph nodes.[13,14] The adverse effects of NPs on the immune system could lead to inflammation, hypersensitivity, immunosuppression, immunostimulation, and autoimmunity. Therefore the interaction between ZnO NPs and immune cells is an important area of research. In addition there are only limited *in vivo* studies, and most of them are focused on the respiratory tract and oral exposure of ZnO NPs.[8,15,16] The release of inflammatory cytokines and imbalance of Th-1/Th-2 cells[17] are induced by ZnO NPs.[18–21] Any change in the cell populations of the immune system (lymphocytes, T-cells, B-cells) is known to cause age-related immune dysfunctions. The studies on inbred laboratory animals have identified age related changes in immunity.[22,23] It is therefore prudent to understand the risk associated with age on treatment with ZnO NPs.

The present study was undertaken to investigate the intraperitoneal toxicity of ZnO NPs. The immunomodulatory effect of ZnO NPs was investigated and their distribution in different tissues was determined. To understand the mechanism of inflammatory response, reactive oxygen species (ROS) was measured by using DCFDA dye in thymocytes. The patho-

[a]*Division of Biological & Life Sciences, School of Arts & Sciences, Ahmedabad University, University Road, Ahmedabad 380009, Gujarat, India. E-mail: ashutosh.kumar@ahduni.edu.in; Fax: +91-79-26302419; Tel: +91-79-26302414*

[b]*CSIR-Indian Institute of Toxicology Research, Vishvigyan Bhavan, 31, Mahatma Gandhi Marg, P.O. Box 80, Lucknow 226001, Uttar Pradesh, India. E-mail: alokdhawan@iitr.res.in*

Downloaded from https://academic.oup.com/toxres/article/6/3/342/5567292 by Ahmedabad University user on 01 May 2025

This journal is © The Royal Society of Chemistry 2017

logical changes induced by ZnO NPs and their possible mechanism of action were also examined.

Experimental

Chemicals

Zinc oxide nanopowder (purity > 99%) used was from Sigma Chemical Co. Ltd (St Louis, MO, USA). A cytometric bead array Kit for TH1/TH2/TH17 cytokines and antibodies (anti-CD3-APC-Cy7, anti-CD4-FITC and anti-CD8a-PE) for immunophenotyping was purchased from BD Biosciences (San Diego, CA, USA). All other chemicals were procured locally and belonged to analytical reagent grade.

Particle characterization

The suspension of ZnO NPs in 0.9% saline was sonicated (Sonics Vibra cell, Sonics & Material Inc., New Town, USA) for 10 min. The average size of ZnO NPs (100 μg mL^{-1}) in Milli-Q water was determined by transmission electron microscopy (TEM; Tecnai™ G2 Spirit, FEI, The Netherlands). The hydrodynamic diameter and zeta potential of ZnO NPs were determined using a Zetasizer Nano-ZS (Malvern instruments Ltd, Malvern, UK). Scanning electron microscopy (SEM; Quanta FEG 450, FEI Company, The Netherlands) was used to observe the particle morphology.

Animals and treatment

Inbred strains of male BALB/c mice [1 month (juvenile), 4 months (adult) and 18 months (aged)] were taken from the animal breeding house of the CSIR, Indian Institute of Toxicology Research (Lucknow, India). Experiments were planned and animals were cared for according to standard guidelines and were approved by the Institutional Animal Ethics Committee. The approval for the experimentation was also taken from the Institutional Animal Ethics Committee. The animals were kept in cages, in animal house and were maintained at a temperature of 23 ± 2 °C, and a humidity of 55 ± 5% under standard laboratory conditions of light and dark cycles (12–12 h). The animals were divided into 9 groups containing 6 mice each (Table 1). Animals were treated with ZnO NPs for 14 consecutive days.

All animals were weighed at the start and end of each treatment. After the treatment, the animals were sacrificed by cervical dislocation.

Table 1 Experimental set up

Groups	Exposure
Juvenile mice	
Group 1	Vehicle control (0.9% saline)
Group 2	ZnO NPs (5 mg per kg b. wt.)
Group 3	ZnO NPs (50 mg per kg b. wt.)
Adult mice	
Group 4	Vehicle control (0.9% saline)
Group 5	ZnO NPs (5 mg per kg b. wt.)
Group 6	ZnO NPs (50 mg per kg b. wt.)
Aged mice	
Group 7	Vehicle control (0.9% saline)
Group 8	ZnO NPs (5 mg per kg b. wt.)
Group 9	ZnO NPs (50 mg per kg b. wt.)

b. wt.: body weight.

Coefficients of liver, spleen and thymus

The coefficients of liver, spleen and thymus were calculated as the ratio of wet weight of tissues to the body weight (b. wt.).

Serum isolation

Blood was collected in dry Eppendorf tubes and was kept at room temperature for 1 h. This led to clotting. Serum was separated by centrifugation at 3000*g* for 10 min and was stored at −80 °C.

Cytokine analysis

The serum samples from control and treated mice were estimated for cytokines using the BD™ cytometric bead array (CBA) mouse TH1/TH2/TH17 Cytokine Kit II according to the protocol described by BD Biosciences (San Jose, CA, USA). Samples were acquired in a flow cytometer (FACSCanto™ II, BD BioSciences, San Jose, CA, USA). The results were analyzed using FCAP Array™ software.[24]

Isolation of thymocytes

The thymus was removed from the BALB/c mice and kept in Roswell Park Memorial Institute (RPMI) 1640 medium. It was minced with tweezers by keeping it on ice to obtain the thymocytes. The isolated thymocytes were passed through a 100 μm nylon mesh filter to remove connective tissue and other lumps. The cells were then centrifuged at 376*g* for 10 min, and further washed twice in RPMI 1640 medium, and the pellet containing thymocytes was resuspended in 1× PBS.

Immunophenotyping

The isolated thymocytes (5×10^6) were suspended in staining buffer (2% FBS in 1× PBS) and stained with APC-Cy7-conjugated anti-CD3, FITC-conjugated anti-CD4 and PE-conjugated anti-CD8 antibodies for 30 min at 4 °C. The stained cells were washed twice with wash buffer (0.2% FBS in 1× PBS). Centrifuged at 350*g* for 5 min and finally suspended in 500 μL ice cold wash buffer. The samples were kept on ice and analyzed within 1 h using a flow cytometer (FACS Canto™ II, BD BioSciences, San Jose, CA, USA). Analysis was done by gating the CD3+ population in a dot plot. The CD3+ population was further resolved into CD4 and CD8 subpopulations.

ROS measurement

ROS was measured as described by Shukla *et al.*[25] The isolated thymocytes (2×10^5) were washed with 1× PBS and suspended in 10 μM of DCFDA for 30 min at 37 °C. Cells were acquired using a flow cytometer (FACS Canto™ II, BD BioSciences, San Jose, CA, USA).[24]

Downloaded from https://academic.oup.com/toxres/article/6/3/342/5567292 by Ahmedabad University user on 01 May 2025

Zn content analysis in different tissues

The Zn content was analysed in tissues of liver, spleen and thymus in all the age groups. The tissue was digested in concentrated nitric acid overnight, to which 5 mL of a mixture of concentrated nitric acid and perchloric acid (6 : 1) was added. The samples were heated at 80–90 °C until the solutions were colourless and clear. The volume of the concentrated solutions was made up to 5 mL with 1% nitric acid. The concentration of zinc in the digested samples was analyzed using an atomic absorption spectrophotometer (AAS; GBC Avanta, Sigma, Australia). The concentration of zinc was expressed as μg per g wet weight of the tissues. Before analysis, AAS was calibrated every time by running standard concentrations (0.25, 0.5 and 1 ppm) of zinc.[8]

Histopathological analysis

The liver, spleen and thymus of control and ZnO NP treated mice were fixed in 10% formalin in PBS for 24–48 h at room temperature. The tissue was dehydrated, cleaned in xylene and embedded in paraffin blocks. Thin sections of tissues (5–8 μm) were obtained and placed onto glass slides which were stained with hematoxylin–eosin and the images were captured using a light microscope (Leica microsystem, Germany).

Transmission electron microscopy

A part of the organ (liver, spleen and thymus) from the control and ZnO NP treated aged mice were cut into small pieces (1 mm) and fixed with 2.5% glutaraldehyde prepared in sodium cacodylate and kept overnight at 4 °C. Further steps were carried out as described in our previous study.[24]

Western blot

For western blot analysis, the liver of control and ZnO NP treated aged mice was taken and homogenized in CelLytic™ M Cell Lysis Reagent (Sigma Chemical Co. Ltd, St Louis, MO, USA) with Na-orthovanadate, Na-fluoride and protease inhibitor cocktail and further centrifuged at 21 000*g* for 30 min at 4 °C, and the supernatant was collected. The estimation of protein was done by the Bradford method.[26] The protocol was performed as described.[24] Proteins were resolved in SDS polyacrylamide gel electrophoresis and were transferred to polyvinylidene fluoride membranes. After blocking of the membrane, the blots were incubated with primary antibodies (1 : 1000) against c-fos, c-jun, nuclear factor kappa B (NF-κB), COX-2, nuclear factor erythroid 2-related factor 2 (Nrf2), phospho-ERK1/2, phospho-JNK, phospho-p38 and γ-tubulin (Abcam, UK) followed by incubation with a secondary anti-primary antibody bound to horseradish peroxidase for 1.5 h at room temperature (Abcam, UK). The protein bands were developed by using ImageQuantLAS 500 software (GE Healthcare Bio-Sciences AB, Sweden). γ-Tubulin served as the protein loading control. Image J software (NIH, USA) was used to quantify the western blot intensity.

Statistical analysis

For comparison between groups, Student's *t*-test and one-way analysis of variance (ANOVA) test were used (using Graph Pad Prism-3.0 Software). $p < 0.05$ and $p < 0.01$ were considered significant.

Results

Particle characterization

ZnO NPs were in the form of white solid nanopowder. The results are described in Table 2. The ZnO NPs were both rod shaped and spherical as observed in SEM. The specific surface area was 15–25 $m^2\ g^{-1}$ (as mentioned by Sigma Chemical Co. Ltd, St Louis, MO, USA).[24]

Coefficients of liver, spleen and thymus

In juvenile and aged mice, significant differences ($p < 0.05$) were observed in the coefficients of thymus and liver respectively at the highest dose of ZnO NPs (50 mg per kg b. wt.). However, no significant changes in the b. wt. of mice of different age groups were observed after 14 days of ZnO NP exposure. Table 3.

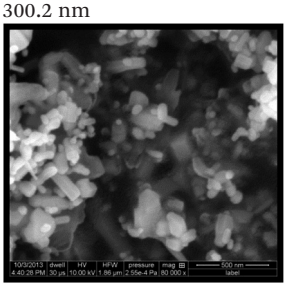
Cytokine analysis

A significant ($p < 0.05$, $p < 0.01$) increase in the levels of inflammatory cytokine (IL-6, IFN-γ and TNF-α) in juvenile and aged mice was observed when exposed to ZnO NPs (50 mg per kg b. wt.). When compared between the age groups of mice, a significant change was observed in aged mice (Fig. 1). Moreover, a significant increase ($p < 0.05$, $p < 0.01$) in the levels of IL-6 and TNF-α was observed in aged mice when compared to juvenile and adult mice as shown in Fig. 1A–C.

Immunophenotyping

No significant change in the percentage of CD3+ cells was observed. However, significant ($p < 0.01$) increase in the number of both CD4- and CD8-cells was observed in aged mice treated with ZnO NPs (50 mg per kg b. wt.) when com-

Table 2 Characterization of ZnO NPs

Properties	ZnO NPs
Average diameter (TEM[a])	~20 nm
Hydrodynamic diameter (DLS[b])	300.2 nm
Shape (SEM[c])	
Purity	99%
Surface area	15–25 $m^2\ g^{-1}$
Zeta potential (DLS[b])	−25.3 mV

[a] Transmission electron microscopy. [b] Dynamic light scattering. [c] Scanning electron microscopy.

Downloaded from https://academic.oup.com/toxres/article/6/3/342/5567292 by Ahmedabad University user on 01 May 2025

This journal is © The Royal Society of Chemistry 2017

Table 3 Effect of ZnO NPs on the mouse body weight and coefficients of liver, spleen and thymus after 14 days of exposure

Groups	Body weight		Liver (mg wet weight per g b. wt.)	Spleen (mg wet weight per g b. wt.)	Thymus (mg wet weight per g b. wt.)
	Before (g b. wt.)	After (g b. wt.)			
Juvenile					
Vehicle control	21.33 ± 0.67	24.67 ± 0.33	58.11 ± 1.29	6.58 ± 0.21	3.58 ± 0.09
ZnO NPs (5 mg per kg b. wt.)	20.67 ± 0.67	23.67 ± 0.88	59.38 ± 1.50	6.95 ± 0.10	3.80 ± 0.07
ZnO NPs (50 mg per kg b. wt.)	20.67 ± 0.67	22.67 ± 0.67	61.79 ± 1.67	7.09 ± 0.04	3.92 ± 0.03*
Adult					
Vehicle control	30.67 ± 0.67	34.67 ± 0.33	54.46 ± 1.34	5.62 ± 0.39	2.32 ± 0.14
ZnO NPs (5 mg per kg b. wt.)	30.33 ± 0.33	33.33 ± 0.88	58.84 ± 0.87	5.89 ± 0.30	2.55 ± 0.04
ZnO NPs (50 mg per kg b. wt.)	30.67 ± 0.67	32.67 ± 0.67	58.89 ± 1.48	5.96 ± 0.21	2.62 ± 0.07
Aged					
Vehicle control	44.67 ± 0.33	48.67 ± 0.67	45.97 ± 1.78	4.10 ± 0.22	1.52 ± 0.05
ZnO NPs (5 mg per kg b. wt.)	44.00 ± 0.58	46.00 ± 0.58	48.02 ± 1.37	4.66 ± 0.06	1.62 ± 0.10
ZnO NPs (50 mg per kg b. wt.)	44.67 ± 0.33	45.67 ± 0.33	53.32 ± 1.39*	4.68 ± 0.26	1.64 ± 0.07

Values represent mean ± standard error of six animals in each group. *$p < 0.05$, when compared with control. b. wt.: body weight.

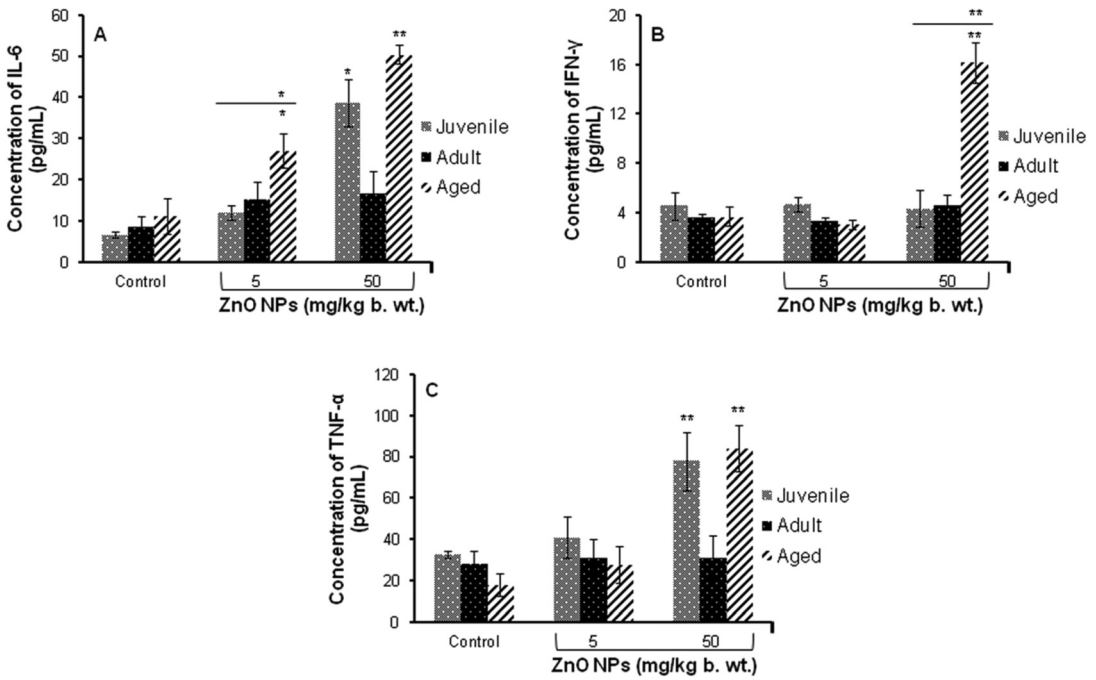


Fig. 1 ZnO NP induced release of cytokines in serum of BALB/c mice (A) IL-6, (B) IFN-γ, (C) TNF-α. Data represents the mean ± S.E.M. of six animals in each group. *$p < 0.05$, **$p < 0.01$ when compared to the control. The horizontal line above indicates a comparison between the different age groups of mice.

pared to the control. Additionally, a significant increase ($p < 0.01$) in both CD4- and CD8- was observed in aged mice when compared to juvenile and adult mice (Fig. 2).

ROS determination

A significant ($p < 0.01$) induction in the release of ROS was observed at the highest dose (50 mg per kg b. wt.) in the thymocytes of juvenile and aged mice compared to the control group. When compared between the three different age groups of mice, a significant ($p < 0.05$, $p < 0.01$) increase in ROS was observed in ZnO NP (5 and 50 mg per kg b. wt.) exposed aged mice (Fig. 3).

Zn content analysis

A significant ($p < 0.05$) increase in the levels of Zn was found in the liver, spleen and thymus of aged mice treated with 50 mg per kg b. wt. ZnO NPs for 14 days when compared to the control. No increase in the Zn content was found in these organs in adult mice while a significant ($p < 0.05$) increase in

Downloaded from https://academic.oup.com/toxres/article/6/3/342/5567292 by Ahmedabad University user on 01 May 2025

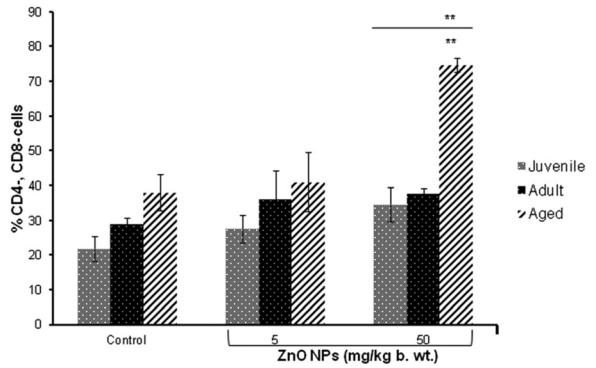


Fig. 2 The bar graph shows the distribution of T cells (CD4- and CD8-) after intraperitoneal exposure of ZnO NPs for 14 days. Data represents mean ± S.E.M. of six animals in each group. $^{**}p < 0.01$ when compared to the control. The horizontal line above indicates a comparison between the different age groups of mice.

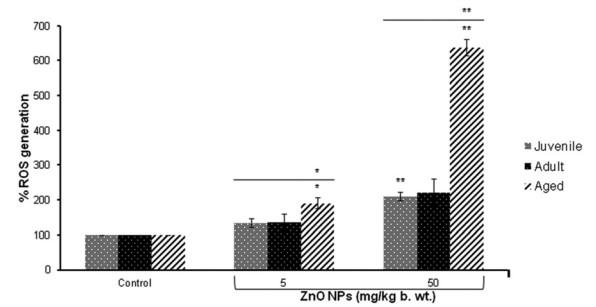


Fig. 3 Release of reactive oxygen species in thymocytes following the intraperitoneal exposure of ZnO NPs for 14 days in BALB/c. Data represents mean ± S.E.M. of six animals in each group. $^{*}p < 0.05$, $^{**}p < 0.01$ when compared to the control. The horizontal line above indicates a comparison between the different age groups of mice.

the Zn content was found only in the liver of juvenile mice (Fig. 4).

Histopathological changes

The liver of juvenile and aged mice exposed to ZnO NPs (50 mg per kg b. wt.) for 14 consecutive days showed pathological lesions (Fig. 5). No changes were observed in the spleen and thymus (data not shown). The infiltration of inflammatory cells like lymphocytes, neutrophils and macrophages was observed in the liver of ZnO NP treated juvenile mice (Fig. 5B) while the liver of ZnO NP treated aged mice revealed vacuole formation and increase in sinusoidal spaces (Fig. 5F). However no pathological alterations were observed in the liver of ZnO NP treated adult mice (Fig. 5D).

Distribution of ZnO NPs and ultrastructural alterations determined by TEM

The accumulation of ZnO NPs and ultrastructural alterations were observed in the cells of liver, spleen and thymus of aged mice exposed to ZnO NPs (50 mg per kg b. wt.) as evident from the electron photomicrographs (Fig. 6). Accumulation of ZnO NPs was seen in the cytoplasm of treated aged mice. ZnO NPs were visible in the hepatocytes as black electron-dense spots along with increase in vacant spaces in the cytoplasm (Fig. 6B).

The splenocytes from untreated control mice show normal cellular features while the splenocytes of ZnO NP administered aged mice show nuclear fragmentation (Fig. 6C and D).

In the thymus of control mice, the thymocytes were closely packed with large nuclei while the ZnO NP administered thymocytes show condensed chromatin, with a deformed nucleus. It also showed irregular cell outlines (Fig. 6E and F).

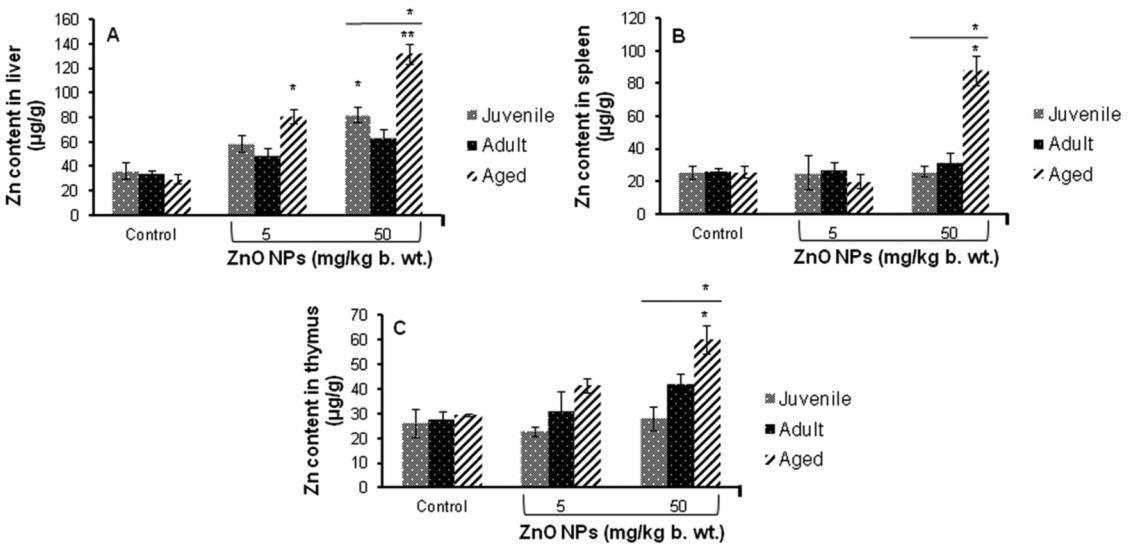


Fig. 4 Zinc content in different tissues of the BALB/c mice after intraperitoneal exposure of ZnO NPs for 14 days, (A) liver, (B) spleen and (C) thymus. Data represents the mean ± S.E.M. $^{*}p < 0.05$, $^{**}p < 0.01$ when compared to the control. The horizontal line above indicates a comparison between the different age groups of mice.

Downloaded from https://academic.oup.com/toxres/article/6/3/342/5567292 by Ahmedabad University user on 01 May 2025

 This journal is © The Royal Society of Chemistry 2017

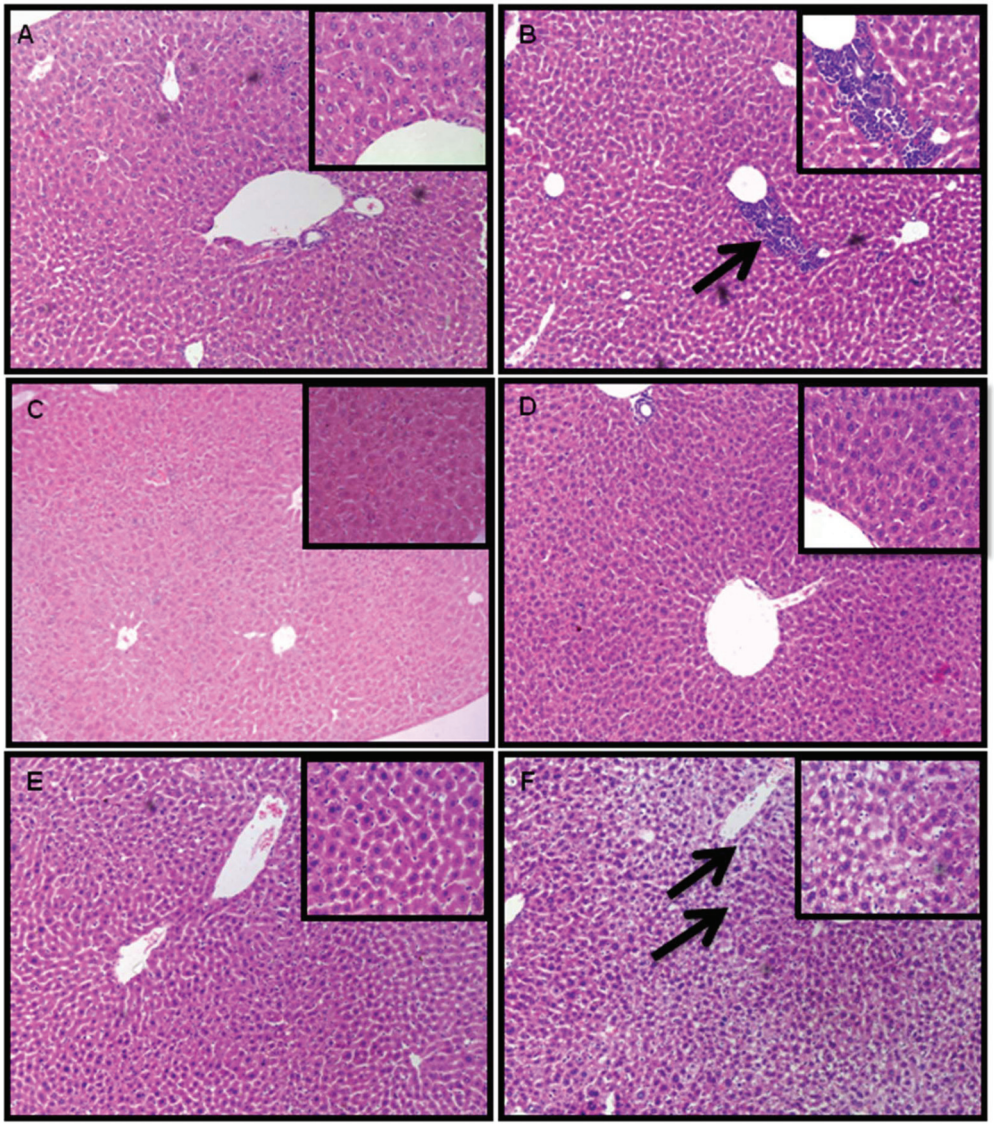


Fig. 5 Histopathological changes in the liver tissue of BALB/c mice after 14 days of intraperitoneal administration of ZnO NPs. (A) Control juvenile group, (B) ZnO NP (50 mg per kg b. wt.) juvenile group, (C) control adult group, (D) ZnO NP (50 mg per kg b. wt.) adult group, (E) control aged group and (F) ZnO NP (50 mg per kg b. wt.) aged group. Sections were stained with hematoxylin and eosin and observed under a light microscope at a magnification of ×100 and ×400 (inset). Pathological alterations are indicated by black arrows.

Western blot analysis

A significant ($p < 0.05$, $p < 0.01$) increase in the levels (1.2–2.5) of inflammatory marker proteins (COX-2) and transcription factor (NF-κB and AP-1 (c-fos and c-jun)) was observed in the liver of aged mice exposed to ZnO NPs (50 mg per kg b. wt.). The expression of the Nrf2 protein was significantly ($p < 0.05$) decreased by ZnO NPs, thereby modulating the antioxidant defence mechanism in the liver (Fig. 7A and B).

A 1.3, 1.8 and 2.4 fold increase in phosphorylated extracellular signal-regulating kinase (ERK1/2), phosphorylated c-Jun N-terminal kinase (JNK) and phosphorylated p38 was observed in ZnO NP treated aged mice (Fig. 7C and D). The expression profile of γ-tubulin was used as an internal control in all the samples.

Discussion

ZnO NPs are known to be cytotoxic and genotoxic *in vitro* and *in vivo*.[8,24,27,28] However, there is a lack of information where the immunomodulatory effects of ZnO NPs are concerned. *In vivo* tests are preferred for the toxicological evaluation as an *in vitro* system cannot mimic the complexity of cell–cell interactions. In the present study, BALB/c mice were chosen as the *in vivo* model due to their immune-competence and similarity with human metabolic, biochemical and physiological pathways.[29]

Understanding the physical and chemical properties of NPs is essential to study the biological effects of the NPs.[30] The mean hydrodynamic diameter of ZnO NPs was 300.2 nm as

Downloaded from https://academic.oup.com/toxres/article/6/3/342/5567292 by Ahmedabad University user on 01 May 2025

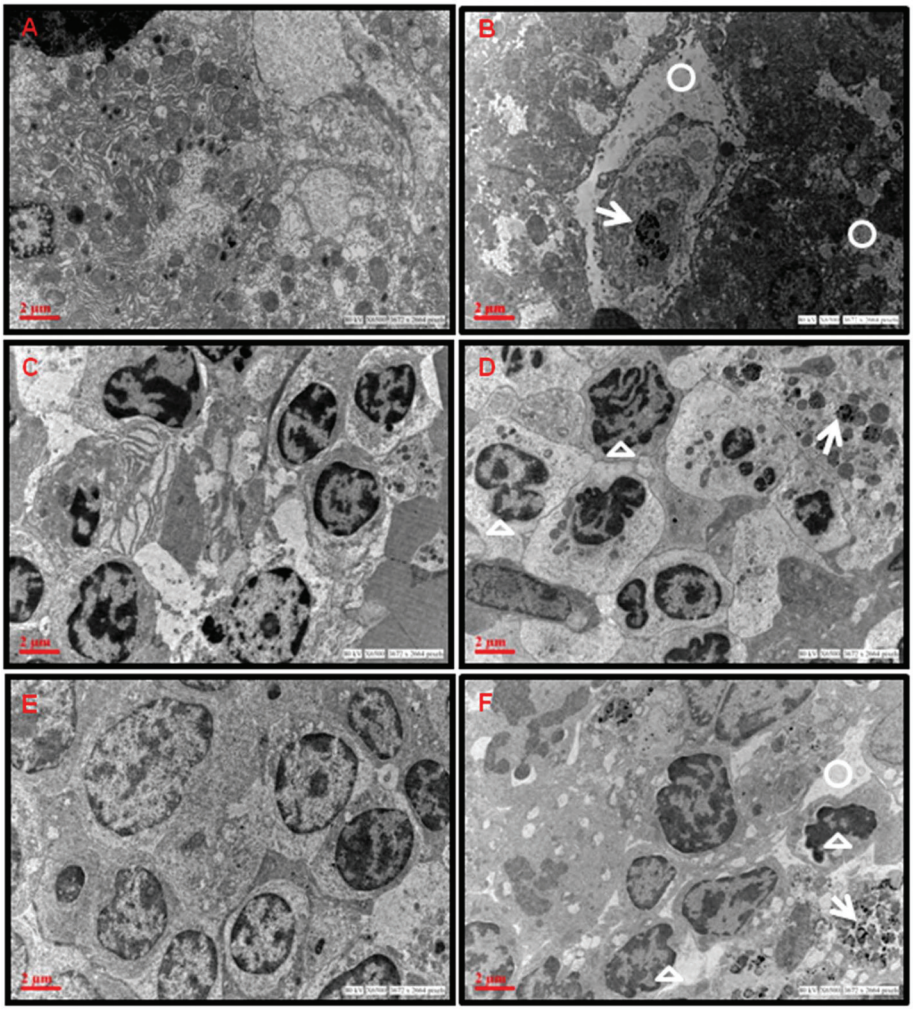


Fig. 6 TEM photomicrographs showing ZnO NP accumulation and ultrastructural changes in aged BALB/c mice administered with ZnO NPs for 14 days. (A) Control liver, (B) ZnO NP (50 mg per kg b. wt.) administered liver, (C) control spleen, (D) ZnO NP (50 mg per kg b. wt.) administered spleen, (E) control thymus and (F) ZnO NP (50 mg per kg b. wt.) administered thymus. White circles indicate increase in vacant spaces in the cytoplasm, white arrows indicate the presence of ZnO NPs and white triangles indicate nuclear fragmentation.

measured by DLS and the average size calculated by TEM was ~20 nm. This difference in sizes is due to the different principles involved in the two measurement techniques.[8,31]

No mortality was observed in either the control or ZnO NP treated BALB/c mice. Moreover no statistically significant difference in b. wt. was observed between the control and treated groups. This suggests that the exposure did not lead to any major visible changes in the health condition of animals.

The immunotoxic potential of ZnO NPs *in vivo* was evaluated by studying the changes in the relative distribution of CD4 and CD8 T cells and cytokine release in the serum. The levels and types of cytokines released determine their role in the regulation of immune responses. The present study showed an increase in IL-6, IFN-γ and TNF-α suggesting the increase in inflammatory cytokines in aged and juvenile mice. The increase of IL-6 and TNF-α indicates the possibility of age-related chronic diseases.[32] IL-6 is an important pro-inflammatory cytokine which mediates T-cell activation.[33] TNF-α plays a role in regulation of immune cells. Hence, its increase denotes a threat to immune functioning *in vivo*. The imbalance between the Th1/Th2 cellular responses leads to the occurrence of many diseases.[16] In the present study, a difference in sensitivity between the Th1 and Th2 responses to ZnO NPs was observed, where the Th1 immunity is observed to be slightly more sensitive. Our data showed that there were no significant changes in the level of IL-2, IL-4 and IL-17 in ZnO NP exposed BALB/c mice of different ages when compared with the control group (data not shown).

The cytokine profile of CD4 cells modulates the functions of the innate and adaptive immune system while CD8 cells cause cytotoxicity and monitor all the cells of the body.[34] Therefore the ratio of CD4/CD8 reflects the immune status of the biological system. Immunophenotyping studies illustrated that ZnO NPs altered the relative proportions of the CD4- and

Downloaded from https://academic.oup.com/toxres/article/6/3/342/5567292 by Ahmedabad University user on 01 May 2025

 This journal is © The Royal Society of Chemistry 2017

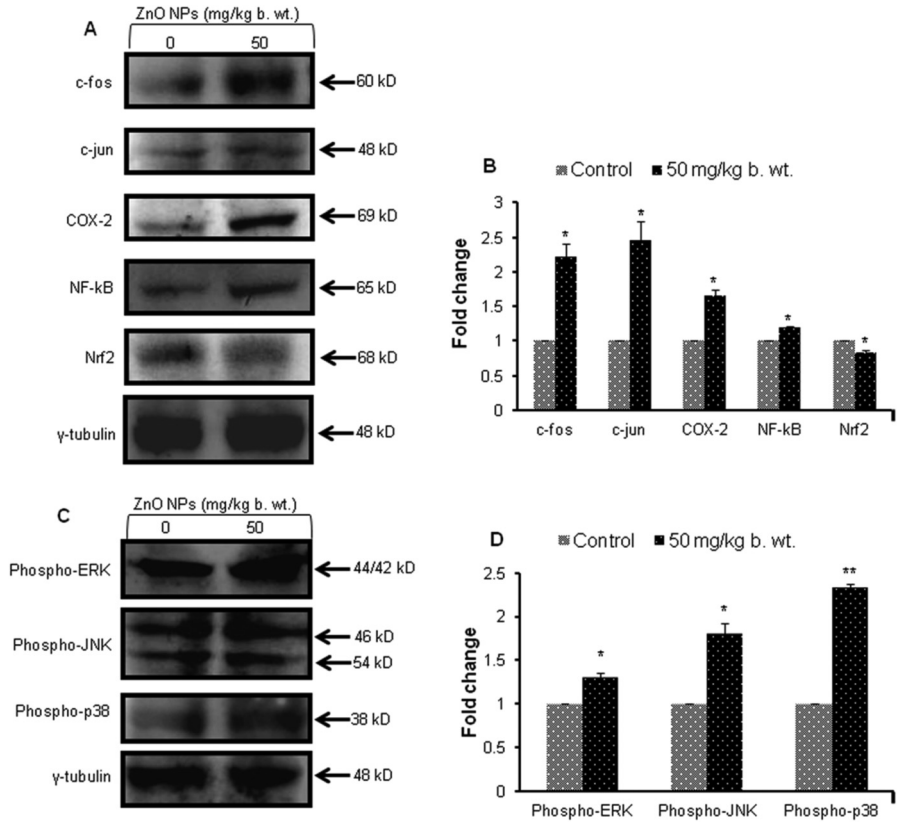


Fig. 7 Western blot analysis of liver proteins from aged mice administered with ZnO NPs (50 mg per kg b. wt.). (A) c-fos, c-jun, COX-2, NF-κB, Nrf2 (C) MAPK signalling proteins (phospho-ERK1/2, phospho-JNK and phospho-p38) and their corresponding bar graphs showing their densitometric analysis (B and D). γ-Tubulin was used as internal control. Data represents the mean ± S.E.M. of three animals in each group. *$p < 0.05$ when compared to the control aged mice.

CD8-T cells with respect to untreated control cells in aged mice. Lymphocyte phenotyping is suggested to be one of the most common indicators of immune cell dysfunction.[35]

Increase in ROS generation was observed in thymocytes of aged mice which indicated that oxidative stress is a key factor in ZnO NP induced toxicity.[36,37] The Nrf2 protein regulates the cellular resistance to oxidants. Our western blot data shows that there is a decrease in the expression of the transcription factor, Nrf2, which clearly indicates that there is an increase in oxidative stress in aged liver tissue on administration of ZnO NPs.[38]

When ZnO NPs find their way into the body, they distribute themselves and get accumulated in different organs due to their small size. The ZnO NPs were found to have a maximum accumulation in the liver of aged mice after a 14 day exposure as observed by AAS data. This was further supported by TEM images where ZnO NPs were observed in the cytoplasm of the hepatocytes of aged mice. The deposited ZnO NPs are responsible for their induced toxicity in aged mice. The ultrastructural changes in the cells from the organs of ZnO NP treated aged mice show deleterious effects of NPs.

Furthermore, the histopathological investigations in the liver of the ZnO NP treated juvenile mice showed the infiltration of inflammatory cells while aged mice revealed vacuole formation and increase in sinusoidal spaces. Due to the intraperitoneal mode of exposure, the ZnO NPs enter the blood and then directly enter the liver. Hence, liver has been observed as one of the primary targets of ZnO NP exposure in both juvenile and aged mice showing pathological changes.[8,39]

Since maximum damage was observed in aged liver tissue compared to the spleen and thymus, the western blot studies were performed for the liver proteins. Our results show an increase in the levels of the COX-2 protein which indicates its induction due to a pro-inflammatory stimulus.[40,41]

The activation of the MAPK signaling pathways was also observed along with the increase in expression of the transcription factor NF-κB.[42,43] Extracellular signal-regulated protein kinases (ERK1/2), c-Jun N-terminal kinase (JNK1/2) and p38 kinases constitute the MAPK proteins. Our results showed that ZnO NP exposure increased the expression of phospho-ERK1/2, phospho-JNK and phospho-p38 in the aged treated mice. Oxidative stress modulates the expression of transcription factors NF-κB and AP-1 (c-fos and c-jun), which further explains the enhanced expression of inflammatory cytokines.

The inflammatory cytokines induce the increased expression of JNK, a major subgroup of MAPK. JNK is activated by MKK4 and MKK7 through phosphorylation on threonine-

Downloaded from https://academic.oup.com/toxres/article/6/3/342/5567292 by Ahmedabad University user on 01 May 2025

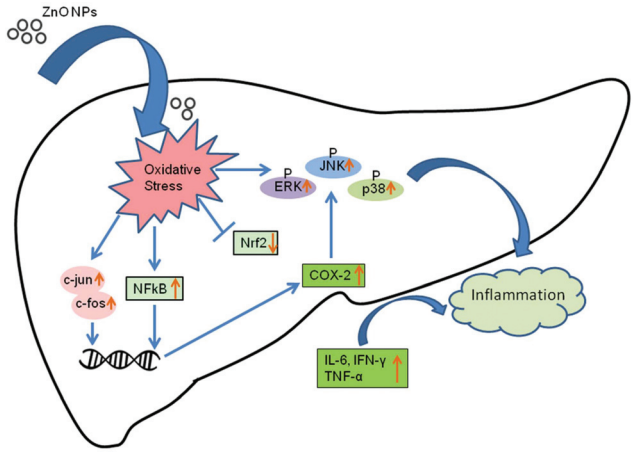


Fig. 8 A schematic showing the possible mechanism of ZnO NP induced inflammatory response in mouse liver cells.

183 and tyrosine-185 residues.[44] The ERK1/2 is induced by growth factors and mitogens through phosphorylation within a conserved threonine–glutamine–tyrosine motif. The protein p38 is also activated by inflammatory cytokines leading to its phosphorylation by MKK3 on threonine-180 and tyrosine-182 which regulate inflammation.[45] Moreover the MAPK signaling cascades also regulate the release of inflammatory proteins such as COX-2. A possible pathway for ZnO NP induced inflammation in mouse liver is shown in Fig. 8.

Conclusions

To our knowledge, this is the first study to report the age dependent immunotoxic effects of ZnO NPs through intraperitoneal administration. The findings of this study demonstrate that, compared to the juvenile and adult mice, the aged mice are more susceptible to ZnO NP induced immunotoxicity. This raises concerns particularly regarding the immunomodulatory effects of NPs in elderly and susceptible populations.

Conflict of interest

The authors do not have any conflicts of interest.

Acknowledgements

Violet A. Senapati is grateful to the Council of Scientific and Industrial Research (CSIR), New Delhi for Junior and Senior Research Fellowship. Funds received from the CSIR, New Delhi, projects NWP35 and NanoSHE (BSC0112), and the EU Framework Programme (FP7/2007-2013; NanoValid-Development of reference methods for hazard identification, risk assessment and LCA of engineered nanomaterials), grant number 263147, is greatly acknowledged. We also acknowledge the Gujarat Institute of Chemical Technology, India (project CENTRA), grant number (ILS/GICT/2013/003) for providing funds.

References

1 R. Langer, Biomaterials in drug delivery and tissue engineering: one laboratory's experience, *Acc. Chem. Res.*, 2000, **33**, 94–101.
2 C. Monteiller, L. Tran, W. MacNee, S. Faux, A. Jones, B. Miller and K. Donaldson, The pro-inflammatory effects of low-toxicity low-solubility particles, nanoparticles and fine particles, on epithelial cells in vitro: the role of surface area, *J. Occup. Environ. Med.*, 2007, **64**, 609–615.
3 A. Nel, T. Xia, L. Madler and N. Li, Toxic potential of materials at the nanolevel, *Science*, 2006, **311**, 622–627.
4 A. Steele, I. Bayer and E. Loth, Inherently superoleophobic nanocomposite coatings by spray atomization, *Nano Lett.*, 2009, **9**, 501–505.
5 H. J. Zhang, B. A. Chen, H. Jiang, C. L. Wang, H. P. Wang and X. M. Wang, A strategy for ZnO nanorod mediated multi-mode cancer treatment., *Biomaterials*, 2011, **32**, 1906–1914.
6 I. F. Osman, A. Baumgartner, E. Cemeli, J. N. Fletcher and D. Anderson, Genotoxicity and cytotoxicity of zinc oxide and titanium dioxide in HEp-2 cells, *Nanomedicine*, 2010, **5**, 1193–1203.
7 V. Sharma, D. Anderson and A. Dhawan, Zinc oxide nanoparticles induce oxidative DNA damage and ROS-triggered mitochondria mediated apoptosis in human liver cells (HepG2), *Apoptosis*, 2012, **17**, 852–870.
8 V. Sharma, P. Singh, A. K. Pandey and A. Dhawan, Induction of oxidative stress, DNA damage and apoptosis in mouse liver after sub-acute oral exposure to zinc oxide nanoparticles, *Mutat. Res.*, 2012, **745**, 84–91.
9 P. G. Rivera, G. Oberdorster, A. Elder, V. Puntes and W. J. Parak, Correlating physicochemical with toxicological properties of nanoparticles: the present and the future, *ACS Nano*, 2010, **4**, 5527–5531.
10 E. Alfaro-Moreno, T. S. Nawrot, B. M. Vanaudenaerde, M. F. Hoylaerts, J. A. Vanoirbeek, B. Nemery and P. H. Hoet, Co-cultures of multiple cell types mimic pulmonary cell communication in response to urban PM10, *Eur. Respir. J.*, 2008, **32**, 1184–1194.
11 B. M. Rothen-Rutishauser, S. G. Kiama and P. Gehr, A three-dimensional cellular model of the human respiratory tract to study the interaction with particles, *Am. J. Respir. Cell Mol. Biol.*, 2005, **32**, 281–289.
12 C. Simona and F. Adriana, In vivo Assessment of Nanomaterials Toxicity, *Nanomaterials*, 2015, 93–121.
13 M. L. Schipper, Z. Cheng, S. W. Lee, L. A. Bentolila, G. Iyer, J. Rao, X. Chen, A. M. Wu, S. Weiss and S. S. Gambhir, microPET-based biodistribution of quantum dots in living mice, *J. Nucl. Med.*, 2007, **48**, 1511–1518.
14 A. K. Mohammad, L. K. Amayreh, J. M. Mazzara and J. J. Reineke, Rapid lymph accumulation of polystyrene

Downloaded from https://academic.oup.com/toxres/article/6/3/342/5567292 by Ahmedabad University user on 01 May 2025

 This journal is © The Royal Society of Chemistry 2017

nanoparticles following pulmonary administration, *Pharm. Res.*, 2013, **30**, 424–434.
15 B. Wang, W. Feng, M. Wang, T. Wang, T. Gu, M. Zhu, H. Ouyang, J. Shi, F. Zhang, Y. Zhao, Z. Chai, H. Wang and J. Wang, Acute toxicological impact of nano- and submicro-scaled zinc oxide powder on healthy adult mice, *J. Nanopart. Res.*, 2008, **10**, 263–276.
16 J. Wang, B. Chen, N. Jin, G. Xia, Y. Chen, Y. Zhou, X. Cai, J. Ding, X. Li and X. Wang, The changes of T lymphocytes and cytokines in ICR mice fed with Fe3O4 magnetic nanoparticles, *Int. J. Nanomed.*, 2011, **6**, 605–610.
17 Y. Liu, F. Jiao, Y. Qiu, W. Li, F. Lao, G. Zhou, B. Sun, G. Xing, J. Dong, Y. Zhao, Z. Chai and C. Chen, The effect of Gd@C82(OH)22 nanoparticles on the release of Th1/Th2 cytokines and induction of TNF-alpha mediated cellular immunity, *Biomaterials*, 2009, **30**, 3934–3945.
18 W. S. Cho, R. Duffin, C. A. Poland, A. Duschl, G. J. Oostingh, W. Macnee, M. Bradley, I. L. Megson and K. Donaldson, Differential pro-inflammatory effects of metal oxide nanoparticles and their soluble ions in vitro and in vivo; zinc and copper nanoparticles, but not their ions, recruit eosinophils to the lungs, *Nanotoxicology*, 2012, **6**, 22–35.
19 M. Giovanni, J. Yue, L. Zhang, J. Xie, C. N. Ong and D. T. Leong, Pro-inflammatory responses of RAW264.7 macrophages when treated with ultralow concentrations of silver, titanium dioxide, and zinc oxide nanoparticles, *J. Hazard. Mater.*, 2015, **297**, 146–152.
20 B. C. Heng, X. Zhao, E. C. Tan, N. Khamis, A. Assodani, S. Xiong, C. Ruedl, K. W. Ng and J. S. Loo, Evaluation of the cytotoxic and inflammatory potential of differentially shaped zinc oxide nanoparticles, *Arch. Toxicol.*, 2011, **85**, 1517–1528.
21 R. Roy, A. Tripathi, M. Das and P. D. Dwivedi, Cytotoxicity and uptake of zinc oxide nanoparticles leading to enhanced inflammatory cytokines levels in murine macrophages: comparison with bulk zinc oxide, *J. Biomed. Nanotechnol.*, 2011, **7**, 110–111.
22 S. C. Castle, Clinical relevance of age-related immune dysfunction, *Clin. Infect. Dis.*, 2000, **31**, 578–585.
23 Y. Wang, Z. Chen, T. Ba, J. Pu, T. Chen, Y. Song, Y. Gu, Q. Qian, Y. Xu, K. Xiang, H. Wang and G. Jia, Susceptibility of young and adult rats to the oral toxicity of titanium dioxide nanoparticles, *Small*, 2013, **9**, 1742–1752.
24 V. A. Senapati, A. Kumar, G. S. Gupta, A. K. Pandey and A. Dhawan, ZnO nanoparticles induced inflammatory response and genotoxicity in human blood cells: A mechanistic approach, *Food Chem. Toxicol.*, 2015, **85**, 61–70.
25 R. K. Shukla, A. Kumar, N. V. Vallabani, A. K. Pandey and A. Dhawan, Titanium dioxide nanoparticle-induced oxidative stress triggers DNA damage and hepatic injury in mice, *Nanomedicine*, 2014, **9**, 1423–1434.
26 M. M. Bradford, A rapid and sensitive method for the quantitation of microgram quantities of protein utilizing the principle of protein-dye binding, *Anal. Biochem.*, 1976, **72**, 248–254.
27 A. Kumar, M. Najafzadeh, B. K. Jacob, A. Dhawan and D. Anderson, Zinc oxide nanoparticles affect the expression of p53, Ras p21 and JNKs: an ex vivo/in vitro exposure study in respiratory disease patients, *Mutagenesis*, 2014, **30**, 237–245.
28 V. Sharma, R. K. Shukla, N. Saxena, D. Parmar, M. Das and A. Dhawan, DNA damaging potential of zinc oxide nanoparticles in human epidermal cells, *Toxicol. Lett.*, 2009, **185**, 211–218.
29 C. A. Argmann, P. Chambon and J. Auwerx, Mouse phenogenomics: the fast track to "systems metabolism", *Cell Metab.*, 2005, **2**, 349–360.
30 K. W. Powers, S. C. Brown, V. B. Krishna, S. C. Wasdo, B. M. Moudgil and S. M. Roberts, Research strategies for safety evaluation of nanomaterials. Part VI. Characterization of nanoscale particles for toxicological evaluation, *Toxicol. Sci.*, 2006, **90**, 296–303.
31 A. Dhawan and V. Sharma, Toxicity assessment of nanomaterials: methods and challenges, *Anal. Bioanal. Chem.*, 2010, **398**, 589–605.
32 T. Singh and A. B. Newman, Inflammatory markers in population studies of aging, *Ageing Res. Rev.*, 2011, **10**, 319–329.
33 P. B. Sehgal, Interleukin-6: molecular pathophysiology, *J. Invest. Dermatol.*, 1990, **94**, 2S–6S.
34 R. V. Luckheeram, R. Zhou, A. D. Verma and B. Xia, CD4(+) T cells: differentiation and functions, *Clin. Dev. Immunol.*, 2012, **2012**, 925135.
35 S. J. Schwulst, J. T. Muenzer, K. C. Chang, T. S. Brahmbhatt, C. M. Coopersmith and R. S. Hotchkiss, Lymphocyte phenotyping to distinguish septic from non-septic critical illness, *J. Am. Coll. Surg.*, 2008, **206**, 335–342.
36 R. Pati, R. K. Mehta, S. Mohanty, A. Padhi, M. Sengupta, B. Vaseeharan, C. Goswami and A. Sonawane, Topical application of zinc oxide nanoparticles reduces bacterial skin infection in mice and exhibits antibacterial activity by inducing oxidative stress response and cell membrane disintegration in macrophages, *Nanomedicine*, 2014, **10**, 1195–1208.
37 M. Saliani, R. Jalal and E. K. Goharshadi, Mechanism of oxidative stress involved in the toxicity of ZnO nanoparticles against eukaryotic cells, *Nanomed. J.*, 2016, **3**, 1–68.
38 Q. Ma, Role of nrf2 in oxidative stress and toxicity, *Annu. Rev. Pharmacol. Toxicol.*, 2013, **53**, 401–426.
39 W. S. Cho, B. C. Kang, J. K. Lee, J. Jeong, J. H. Che and S. H. Seok, Comparative absorption, distribution, and excretion of titanium dioxide and zinc oxide nanoparticles after repeated oral administration, *Part. Fibre Toxicol.*, 2013, **10**, 9.
40 E. J. Park, J. Roh, Y. Kim and K. Park, Induction of Inflammatory Responses by Carbon Fullerene (C60) in Cultured RAW264.7 Cells and in Intraperitoneally Injected Mice, *Toxicol. Res.*, 2010, **26**, 267–273.

Downloaded from https://academic.oup.com/toxres/article/6/3/342/5567292 by Ahmedabad University user on 01 May 2025

41 C. Tsatsanis, A. Androulidaki, M. Venihaki and A. N. Margioris, Signalling networks regulating cyclooxygenase-2, *Int. J. Biochem. Cell Biol.*, 2006, **38**, 1654–1661.
42 Y. Lu and L. M. Wahl, Oxidative stress augments the production of matrixmetalloproteinase-1, cyclooxygenase-2, and prostaglandin E2 through enhancement of NF-Kappa B activity in lipopolysaccharide-activated human primary monocytes, *J. Immunol.*, 2005, **175**, 5423–5429.
43 J. Wang, X. Deng, F. Zhang, D. Chen and W. Ding, ZnO nanoparticle-induced oxidative stress triggers apoptosis by activating JNK signaling pathway in cultured primary astrocytes, *Nanoscale Res. Lett.*, 2014, **9**, 117.
44 Y. Fleming, C. G. Armstrong, N. Morrice, A. Paterson, M. Goedert and P. Cohen, Synergistic activation of stress-activated protein kinase 1/c-Jun N-terminal kinase (SAPK1/JNK) isoforms by mitogen-activated protein kinase kinase 4 (MKK4) and MKK7, *Biochem. J.*, 2000, **352**, 145–154.
45 D. K. Morrison, MAP Kinase Pathways, *Cold Spring Harbor Perspect. Biol.*, 2012, **4**, a011254.

Downloaded from https://academic.oup.com/toxres/article/6/3/342/5567292 by Ahmedabad University user on 01 May 2025

This journal is © The Royal Society of Chemistry 2017